Evaluation of poly-β-hydroxybutyrate as a sorbent material for the removal of spilled crude oil from water

Junfeng Dou, Jing Yuan, Aizhong Ding, En Xie, Shuairan Li, Lei Zheng*

College of Water Sciences, Beijing Normal University, Beijing 100875, China, Tel. +86 10 58802739, emails: doujf@bnu.edu.cn (J. Dou), xyvy-8945@163.com (J. Yuan), ading@bnu.edu.cn (A. Ding), hippo668@163.com (E. Xie), lishuairan2007@163.com (S. Li), zhengleilei@bnu.edu.cn (L. Zheng)

ABSTRACT

Oil spills in the ocean are becoming an increasingly serious problem and the search for an adsorption material that is effective and environmentally safe is a popular research topic. This study presents a sorbent micro-ball composed of poly-β-hydroxybutyrate. Field emission scanning electron microscopy was used to observe morphology of the micro-ball. Additionally, Fourier transform infrared spectroscopy was used to analyze the surface groups, and nitrogen adsorption was used to determine specific surface area and pore size distribution. The effects of such conditions as initial oil concentration, temperature, pH, and water salinity on the adsorption efficiency were studied. The results show that the equilibration time is 60 min. The adsorption isotherm experiments indicate that the Freundlich model fits the experimental data better than the Langmuir and Henry models, and the adsorption kinetics experimental results show that the pseudo-second-order model fits the experimental data well. The adsorption capacity is proportional to the initial oil concentration. The removal rate increases as the temperature increases, and the adsorption efficacy is highest at a temperature of 25℃. The adsorption capacity varies directly with pH value. Finally, the adsorption capacity of micro-balls increases with increasing seawater salinity.

Keywords: Oil spill pollution; PHB; Sorbent preparation; Adsorption properties; Removal rate

1. Introduction

Increasing tourism as well as oil transport and exploration elevate the risk of oil spills at sea [1] In 1989, more than 41,000 m^3 of crude oil was discharged by the *Exxon Valdez* into the waters of Prince William Sound, Alaska, polluting at least 2,000 km of shoreline [2,3]. In 2002, the oil tanker *Prestige* sank, spilling approximately 60,000 tons of heavy fuel oil and affecting much of the Galician coast, the Cantabrian coast, and the southern portion of the Bay of Biscay [4,5]. In 2010, an estimated 780,000 m^3 of crude oil leaked into the Gulf of Mexico in the *Deepwater Horizon* oil spill [6–8]. Indeed, similar cases in recent years are too numerous to list. One example of a case requiring the rapid removal of crude oil is the oil tank explosion that occurred in 2010 near Dalian, China, in which damaged pipes released an estimated 1,500 tons of crude oil into the nearby harbor and the Yellow Sea.

Oil consists of such compounds as alkanes and polycyclic aromatic hydrocarbons, which are toxic,

*Corresponding author.

carcinogenic, and teratogenic to human beings. Although they can weather relatively quickly (over years) or slowly (over decades or even longer), oil spills can have widespread, long-term effects on the ecological world on which human rely. Oil spills generally affect coastal wetland plants, reducing photosynthesis, transpiration, shoot height, stem density, biomass, growth, and regrowth, and even cause complete mortality depending upon the oil type, degree of weathering, spill volume, mode of contact with the vegetation, penetration of the soil, and other factors [7]. In addition, the oil film, which affects water reaeration, results in the larger scale death of organisms due to a lack of oxygen. Furthermore, the toxic compounds are transported into humans by bioaccumulation. Ultimately, oil spills are one of the main factors contaminating ocean environments. Thus, the development of methods to remove contamination from the ocean and ameliorate the aquatic environment is an important research topic.

Generally, methods dealing with oil spill are related to physical removal, chemical degradation and bioremediation. Physical removal is an easy, low cost, and highly efficient removal method without secondary pollution [9,10]. However, it is limited to several specific conditions related to the oil characteristics, the spill volume, and the location of the accident, among other factors. In chemical degradation studies, it is common to investigate the photochemical process of the degradation [11,12]. However, the chemicals added to the environment to induce degradation may cause secondary pollution. Compared to the first two methods, bioremediation is safer, more economical, and more effective [13,14]. Nevertheless, bioremediation is a relatively slow approach. Therefore, the development of a sorbent that can be degraded by micro-organisms is of great interest. This study attempts to address this issue.

The sorbent materials used for oil spill cleanup include organic materials, such as vegetable fibers, straw, kapok, and sawdust [15–18]; synthetic organic materials, such as polypropylene and polyurethane; and inorganic materials [19]. Few studies investigate biodegradable materials in this context. The characteristics of poly-β-hydroxybutyrate (PHB) are similar to those of petrochemically produced polypropylene, with the added advantage of biodegradability. In addition to serving as a biodegradable material, PHB has recently been applied in the manufacturing of high-performance materials.

In the present study, PHB was applied to prepare a biomimetic adsorbent micro-ball, and electron microscopy and infrared spectroscopy were used to characterize the micro-balls. The removal efficiency of this material for spilled crude oil from Dalian seawater was also evaluated.

2. Material and methods

2.1. Seawater samples

Seawater samples were taken from Dalian Xingang oilport and stored at 4°C for transportation. Dalian Xingang oil port is located in the southern end of Liaotung Peninsula, on the west coast of Dayao Bay in the Yellow Sea, China. On 16 July 2010, an explosion occurred at Dalian Xingang oilport, which destroyed approximately 200 m of oil pipeline, caused a serious oil fire, combusted over 100,000 m^3 of crude oil and created significant air pollution. This explosion resulted in the release of over 1,500 tons of crude oil into the Yellow Sea, creating a potential disaster for the marine environment and ecology. The seawater salinity of Dalian is 20.16 g/L.

2.2. Sorbent preparation

2.2.1. Chemicals

PHB, whose melting temperature (T_m) is 172°C, was purchased from Haiyun Co. (Tianjin, China). Chloroform was purchased as analytical standard from Beijing Chemical Plant (China). The mass fraction of the formaldehyde is 37%, while the density of chloroform is 20 g/mL (20°C).

2.2.2. Sorbent ball preparation

The sorbents were prepared using the method of double-emulsion water-in-oil-in-water (W_1/O/W_2) solvent evaporation. The reagents and dosages used in the preparation are shown in Table 1, and the process is depicted in Fig. 1.

First, PHB was completely dissolved in chloroform under constant stirring (O). Second, deionized water (W_1) was added into the oil phase (PHB and chloroform) under even and constant stirring to obtain the primary emulsion (W_1/O). Then, the primary emulsion was then diluted using the appropriate volume of

Table 1
Reagents and dosages used in sorbent ball preparation

Phase	Components	Amount
W_1	UF suspension liquid	12 mL
O	PHB	6.6 g
	Chloroform	50 mL
W_2	Deionized water	300 mL
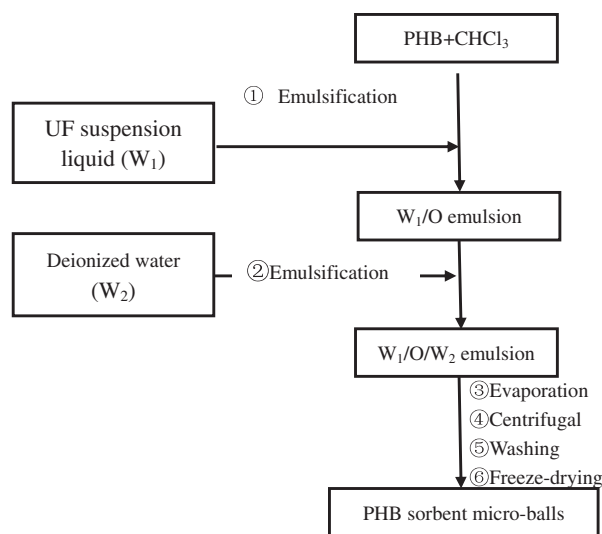
Fig. 1. Diagram of sorbent ball preparation. ①, ②, ③, ④, ⑤, and ⑥ refer to the operation order.

deionized water (W_2) to obtain the double emulsion ($W_1/O/W_2$), which was stirred to evaporate the chloroform and solidify the PHB sorbent micro-balls. Finally, the PHB particles were filtered and freeze-dried for 24 h.

2.3. Characterization methods

The surface and cross section of the PHB sorbent micro-balls were investigated by field emission scanning electron microscopy (FE-SEM) (S-4800, Hitachi Ltd, Japan). Samples were freeze-dried for 24 h and sputter-coated with gold prior to imaging.

The specific surface area and pore size distribution of the sorbent micro-balls were measured using a Nove2000e instrument from Quantachrome Co. (USA). The samples were degassed at 90℃ and then subjected to N_2 adsorption experiments at 77.4 K.

The surface groups of the PHB sorbent micro-balls were analyzed by Fourier transform infrared spectroscopy and Raman spectroscopy (Nexus 670, Nicolet, America). Samples were ground in liquid nitrogen, mixed with Fourier transform infrared spectroscopy (FT-IR)-grade KBr and pelletized.

2.4. Adsorption of pure diesel oil

Diesel oil was chosen to analyze the adsorption efficiency of the micro-balls. A sample of micro-balls (0.3 g) was added to 10 mL of pure diesel oil, stirred at 98 r/min, removed after 10 min, and weighed. The adsorption of pure diesel oil, q(g/g), was calculated using Eq. (1):

$$q = \frac{(M_2 - M_1)}{M_1} \qquad (1)$$

where M_1 (g) and M_2 (g) are the micro-ball weights at time 0 and 10 min, respectively.

2.5. Adsorption of dissolved diesel oil

For each adsorption isotherm experiment, 20 mL of diesel oil aqueous solution containing 0.1 g of the micro-balls was stirred at 130 r/min under constant temperature. The nine different concentrations of diesel oil studied ranged from 0.50 to 40.50 g/L. The equilibration time was 60 min, which was determined in a preliminary study. After attaining equilibrium, the oil phase was separated to measure the concentration of the diesel oil.

The initial concentrations of diesel oil employed in the kinetics experiments were 17, 8.5, and 4.25 g/L. A series of conical flasks with 20 mL of diesel oil solution and 0.1 g of the micro-balls were stirred at 130 r/min. At predetermined time intervals, the solutions were separated to measure the concentration of diesel oil.

2.6. Effects of different conditions on the adsorption

The oil concentration varies depending on the characteristics of the water samples of interest; thus, the adsorption would be affected by the oil concentration. To study this effect, 20 mL of different concentrations of diesel oil aqueous solutions containing 0.1 g of the micro-balls was stirred at 130 r/min under the conditions of 25℃ and pH 6. At the equilibration time (60 min), the solution was extracted with n-hexane twice, and the absorption was measured at 225 nm. The removal rate of the oil and adsorption per adsorbent were then calculated.

Temperature and pH affect the adsorption efficacy. In this study, temperatures of 15, 20, and 25℃ and pH values of 6, 8, and 9 were used to determine the effects of temperature and pH on the adsorption.

Seawater salinity affects the adsorption of non-ionic organic pollutants. Saturated mixtures of diesel and seawater were divided into six groups with a salinity gradient ranging from 1 to 25 g/L. The volume of the mixture solution was 20 mL, and the mass of the micro-balls for each sample was 0.1 g. The other conditions used in the adsorption experiment were the same as above.

2.7. Analytical method

The adsorption of pure diesel oil was determined by the gravimetric method. The concentration of diesel

oil was determined by UV–vis spectrophotometry, and analytically pure n-hexane was chosen as the solvent. A characteristic absorption peak was observed at a wavelength of 225 nm. The absorbance is proportional to concentration, and n-hexane was selected as the reference fluid. The calibration curve was established by injecting eight standard solutions with concentrations of 1, 2.5, 5, 8, 10, 25, 50, and 100 µg/mL, yielding a fitting coefficient (R^2) of 0.999.

3. Results and discussion

3.1. Characteristics of the sorbents

3.1.1. Morphological identification

PHB is a powder and cannot be used as adsorbent because it cannot be collected from water. In contrast, micro-balls prepared from PHB are porous spherical particles, as shown in Fig. 2. The surface and cross

Fig. 2. External appearance of the micro-balls.

section of a representative micro-ball are shown in Fig. 3. SEM images show that the micro-ball has a rough surface and a microporous interior. The micro-balls have a wide pore size distribution, with diameters ranging from 3 to 100 nm. Furthermore, the specific surface area of the balls is 18.840 m^2/g, the pore volume is 0.033 cm^3/g, and the average pore diameter is 4.100 nm. The high surface area and good dispersibility and separation performance of the micro-balls make them suitable adsorbents. Zhang et al. prepared a biomimetic adsorbent using PHB called PHBBMA, and reported that its specific surface area and pore volume are 8.45 m^2/g and 0.0105 cm^3/g, respectively [20], which are lower than those of the micro-balls prepared in this study.

The micro-ball pores were created by the vaporization of chloroform; thus, the pore diameter was influenced by the concentration of PHB in chloroform and the volume ratio of chloroform and deionized water, among other factors. In contrast, the micro-ball particle size was determined by the stirring speed, with faster stirring creating smaller micro-balls. Therefore, the optimization of the micro-ball properties can be achieved by controlling the experimental conditions.

3.1.2. Functional group identification

The surface groups of the micro-balls were analyzed by FT-IR spectroscopy. As shown in Fig. 4, the most prominent absorption bands were ascribed to C=O (1,721 cm^{-1}, stretch), methyl (2,875 and 2,977 cm^{-1}, stretch), methylene (2,934 cm^{-1}, stretch), methyl (1,383 cm^{-1}, bending), methylene (1,458 cm^{-1}, bending), C–O–C (1,181 cm^{-1}, stretch), and methylidyne (1,290 cm^{-1}, stretch). Based on the results reported by Zhang [21], the FT-IR spectrum of the micro-balls was in accordance with that of PHB. The results also proved that the preparation of the micro-balls is a physical process.
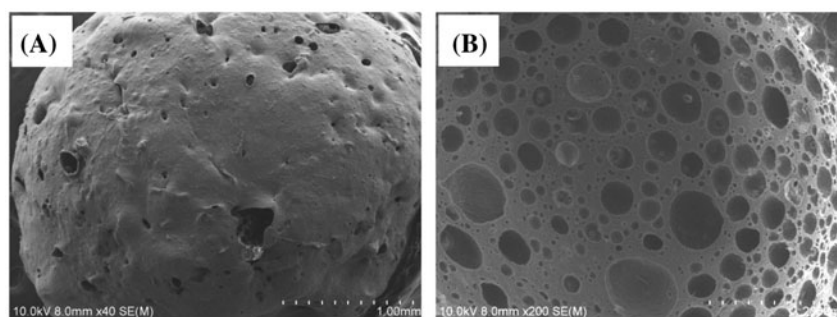
Fig. 3. Scanning electron micrographs of a micro-ball: (A) surface and (B) cross section.
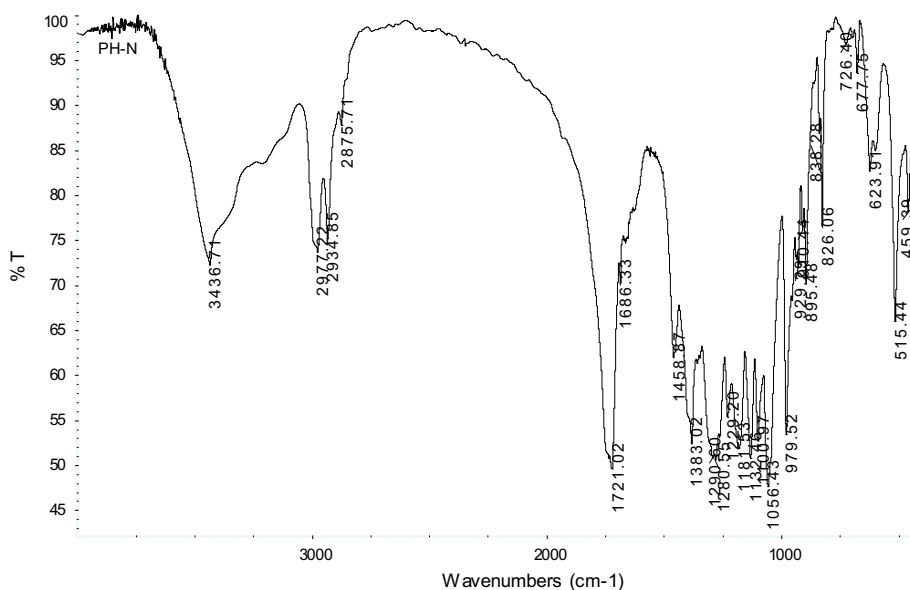
Fig. 4. Micro-ball FT-IR spectrum.

3.2. Adsorption characteristics

3.2.1. Adsorption isotherm experiments

The results for the adsorption of pure diesel oil, shown in Table 2, indicate that adsorption saturation can be achieved in 60 min. The adsorption of the micro-balls is 1.8 g/g, while that of PHB is 0.8 g/g. It is suggested that the morphological and textural characteristics contribute to the capacity of the micro-balls. Cao and Qin studied the adsorption properties of diesel oil on exfoliated graphite and found that the greater the expansion volume is, the greater the maximum adsorption capacity [22]. The results show that the maximum adsorption capacity of exfoliated graphite is greater than 22 g/g at room temperature. Zhou et al. used kapok fiber as a natural sorbent for the removal of oil from water, reporting an equilibration time of 4 h and a maximum adsorption capacity of 25 g/g [23]. Based on the results of these studies, the optimization of the adsorption properties of micro-balls will be the subject of future work.

The adsorption isotherms for the adsorption of diesel oil from aqueous solution onto the micro-balls are shown in Fig. 5. The adsorption per unit mass adsorbent, Q (g/g) was calculated using Eq. (2):

$$Q = \frac{V(S_1 - S_0)}{M} \tag{2}$$

where S_0 (g/L) and S_1 (g/L) are the concentrations of diesel oil in the solution at time 0 and 60 (min), respectively; V (L) is the solution volume; and M (g) is the dose of the adsorbent. The curve in Fig. 5 depicts Q. The experimental data were analyzed using the Langmuir, Freundlich, and Henry models, and the fitting results are presented in Fig. 6 and Table 3.

The Langmuir equation is employed for homogeneous surfaces. Based on this equation, the adsorption capacity of the micro-ball is 1.90 g/g, which deviates substantially from the experimental value (2.56 g/g),

Table 2
Pure diesel oil adsorption of different adsorbents

Sample	Mass (g)	Adsorption (g/g)
PHB	0.3109	0.8
Micro-balls	0.3014	1.8
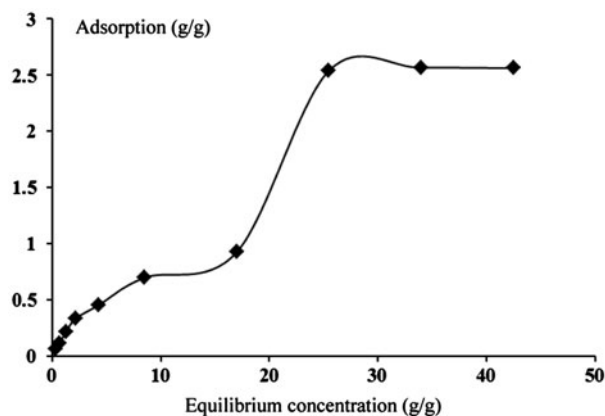
Fig. 5. Adsorption isotherm for micro-balls.
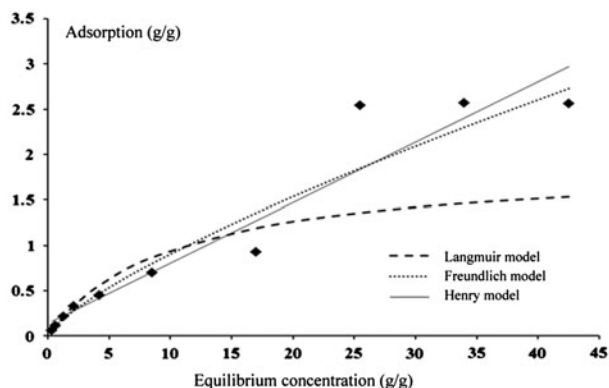
Fig. 6. Fitting results for adsorption isotherm curves.

Table 3
Fitting results for adsorption isotherms equations

Name	Adsorption isotherms	R^2
Langmuir	$1/C_s = 5.156/C_e + 0.339$	0.995
Freundlich	$\lg C_s = 0.809 \lg C_e - 0.759$	0.988
Henry	$C_s = 0.2106 + 0.0793 Ce$	0.926

as shown in Fig. 6. Although its R^2 value (0.997) in Table 3 is higher than those of the other models, this deviation indicates that the Langmuir equation cannot fit the experimental data well. The Langmuir model is widely employed in monolayer adsorption. At its maximum adsorption capacity, the pores of the micro-ball adsorbent are filled with the adsorbate molecules, preventing the micro-ball from adsorbing additional molecules. This adsorption process, micro-pore adsorption, differs from monolayer adsorption. Therefore, the Langmuir equation is not appropriate for describing the adsorption of the micro-ball from a theoretical standpoint.

The Freundlich isotherm began as an empirical equation but was later interpreted theoretically. This equation can be given as Eq. (3):

$$q_e = K_f C_e^{1/n} \tag{3}$$

where K_f and n are indicators of the adsorption capacity and intensity, respectively. The higher n is, the better the adsorption capacity. The sorption isotherm is a linear curve when $n = 1$. When $n < 1$, the adsorption curve bends downward, indicating that as the adsorbate concentration increases, the energy of the adsorption increases and the adsorption weakens. When $n > 1$, the behavior is opposite. The Freundlich model fitted the experimental data well, as indicated in both Fig. 6 and Table 3 ($R^2 = 0.978$).

The Henry model, for which the R^2 value was lower than that of the other models, could not fit the experimental data well. It is most applicable when strong adsorption sites are present in low concentrations and saturation is far from being achieved. However, in the case of the micro-balls, the adsorption achieves saturation. This conclusion is also supported by the results in Fig. 6.

3.2.2. Adsorption kinetics experiments

To evaluate the rate of the adsorption, which is one of the key factors in practical applications, the adsorption kinetics were studied. The kinetic curves are shown in Fig. 7.

The rates of adsorption for different oil concentrations are initially rapid, later slowing until reaching the adsorption equilibrium. The equilibration time is approximately same for the various oil concentrations
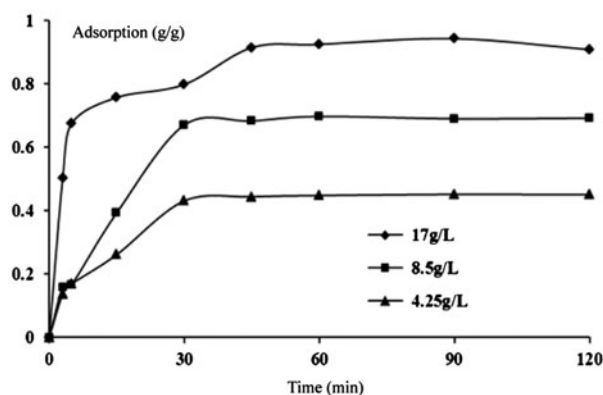
Fig. 7. Diesel oil adsorption kinetics on micro-balls.
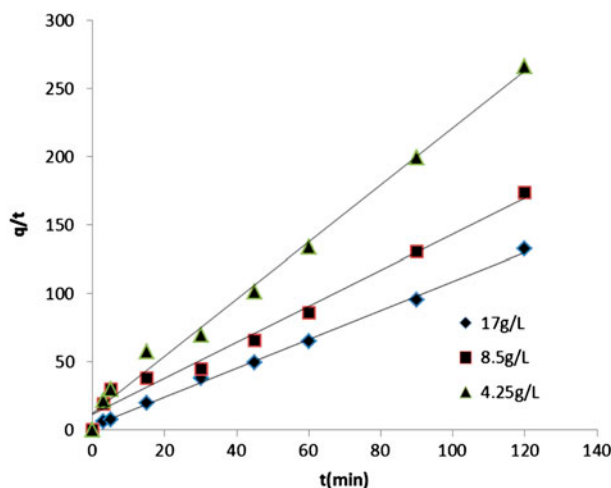
Fig. 8. Fitting results for adsorption kinetics curves.

Table 4
Fitting results for adsorption kinetics data

Concentration/g L^{-1}	Trend line	Q/mg g^{-1}	K/g (min g)$^{-1}$	R^2	T/min
17	t/q = 1.057t + 2.927	0.9460	0.3817	0.998	52.80
8.5	t/q = 1.277t + 14.67	0.7830	0.1111	0.987	218.2
4.25	t/q = 2.040t + 16.00	0.4901	0.2594	0.994	149.4

(approximately 60 min). In addition, Fig. 7 shows that the higher the initial concentration, the greater the adsorption.

The kinetics can be described by the pseudo-second-order model as

$$\frac{t}{q_t} = \frac{1}{k\,q_2^2} + \frac{1}{q_2}t \qquad (4)$$

where q_2 (g/g) is the equilibrium adsorption; q_t (g/g) is the adsorption at time t; and k (min^{-1}) and t (min) are the rate constant of the second-order sorption and the adsorption time, respectively. The fitting results for the curve and data are shown in Fig. 8 and Table 4. The value of R^2 for the fit to different concentrations is above 0.987, indicating that the pseudo-second-order model fits the experimental data well. Yang et al. studied the biomimetic adsorption of polycyclic aromatic hydrocarbons, reporting that the pseudo-second-order model describes the adsorption of naphthalene, phenanthrene, and pyrene better than the pseudo-first-order model [24].

3.3. Effects of different conditions on the adsorption

3.3.1. Effects of initial oil concentration on the adsorption

Fig. 9 indicates that the removal rate of the oil decreased as the initial oil concentration increased, whereas the adsorption capacity had a positive effect on the initial oil concentration. This result is explained by the fact that the higher the initial oil concentration is, the closer it is to the maximum adsorption capacity. When the oil concentration is 0.3 g/L, the oil removal rate of the micro-ball is above 90%, and when the initial oil concentration is 42.5 g/L, the adsorption per adsorbent is 2.57 g/g.

3.3.2. Effects of temperature on the adsorption

Fig. 10 demonstrates that the removal rate increased as the temperature increased and the adsorption efficacy was the highest when the temperature was 25°C. It
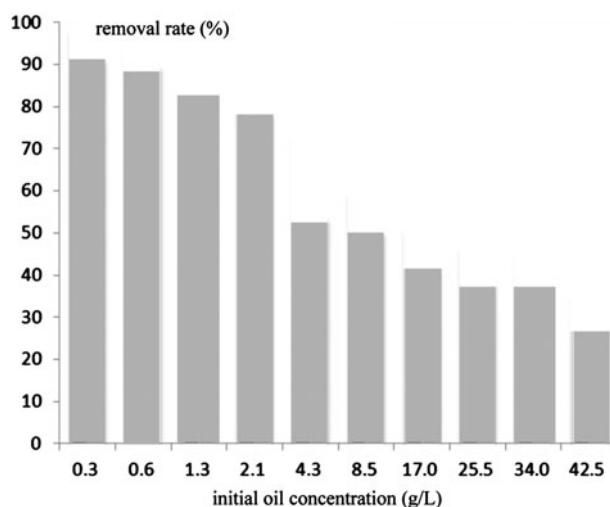
Fig. 9. Oil removal rate for different initial oil concentrations.
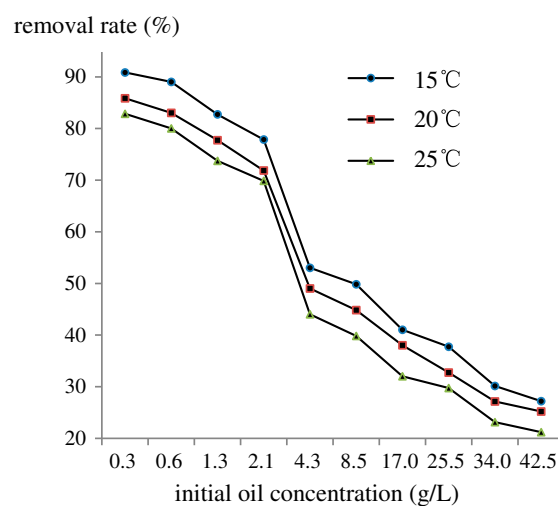
Fig. 10. Oil removal rate at different temperatures.

can be concluded that high temperatures strengthen the efficacy of oil removal. On the one hand, high temperatures increase the activation energy of the micro-ball adsorbent, increasing its probability of colliding

with the oil molecules. On the other hand, at high temperatures, the oil viscosity decreases and its fluidity increases, again promoting the collision between oil molecules and the adsorbent. Thus, high temperatures increase the removal rate of oil. Lin found that the adsorption of oil decreased about 9% while the adsorption of water decreased about 12% by the modified expanded perlite balls during 10–25°C [24].

3.3.3. Effects of pH on the adsorption

Fig. 11 shows that the pH had a positive effect on adsorption capacity. Under weak acidic conditions, H$^+$ can neutralize the negative charges on the surface of the oil molecules, thereby destabilizing them. Oil molecules with low stability tend to aggregate on the surface of the adsorbent, increasing the adsorption amount. As the pH increases, the inorganic bases in water and organic acids react with surface-active substances, decreasing the viscosity of the oil and promoting dispersion. Meanwhile, OH$^-$ increases the repulsive force between the surfaces of the adsorbent and oil molecule, decreasing the adsorption of the micro-ball. Yang et al. studied the effect of pH on the adsorption of naphthalene, phenanthrene, and pyrene, finding no significant effect on the adsorption [25]. This lack of effect is because PAHs are non-ionic organic compounds, supporting the results of this study.

3.3.4. Effects of water salinity on the adsorption

Fig. 12 shows that the adsorption amount increases with the water salinity. The salinity influences the
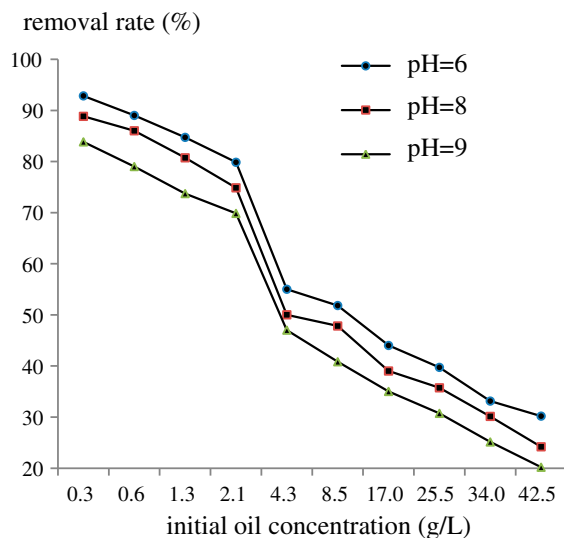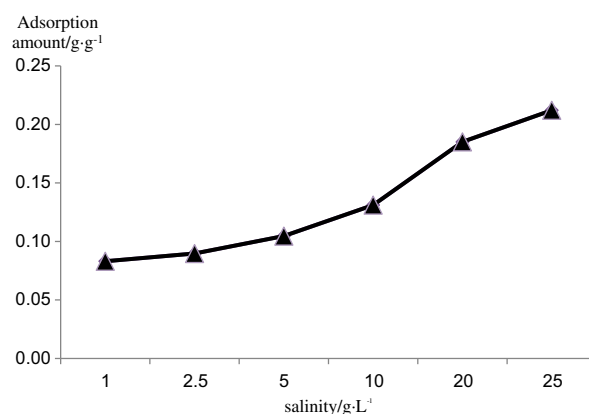
Fig. 12. Oil adsorbed in different salinities.

adsorption process by affecting the properties of the diesel solution. The water solubility of diesel decreases with increasing water salinity, and the solvable part of diesel on the micro-balls would be salted out at elevated salinity. Therefore, the adsorption capacity of micro-balls increases with increasing seawater salinity. Yin found that the adsorption of dissolved oil increased by sand soil with increasing salinity, and the reason for which was that increasing salinity strengthened the ionic strength, which promoted the adsorption of dissolved oil into sand soil [26].

4. Conclusions

Micro-balls prepared with PHB by double-emulsion solvent evaporation are a promising friendly adsorbent for removing spilled crude oil from water. The FE-SEM images of the micro-balls reveal that they are porous spherical particles, which contributes to their high adsorption ability. The adsorption isotherm results show that the Freundlich model fits the experimental data better than the Langmuir and Henry models. The adsorption kinetics results show that the pseudo-second-order model fits the experimental data well. The results show that physical and chemical mechanisms are both in the adsorption process of micro-balls, while the former is the main mechanism. This study also found that the removal rate of the oil decreased as the initial oil concentration increased, while the initial oil concentration had a positive effect on adsorption capacity. The removal rate increased with temperature, and the adsorption efficacy was the highest at 25°C. In addition, the pH had a positive effect on the adsorption capacity, with pH 6 being optimal in this study. The diesel adsorption capacity of the micro-balls and the seawater salinity are positively related, and the improvement of the adsorption

Fig. 11. Oil removal rate at different pH values.

ability in high-salinity seawater requires further research. The results of the study show that the micro-balls effectively and quickly adsorb not only the oil film on the sea but also the oil diluted in the sea.

References

[1] C.M.B. Jaraula, F. Kenig, P.T. Doran, J.C. Priscu, K.A. Welch, Composition and biodegradation of a synthetic oil spilled on the perennial ice cover of Lake Fryxell, Antarctica, Environ. Sci. Technol. 43 (2009) 2708–2713.

[2] P.D. Boehm, D.S. Page, J.S. Brown, J.M. Neff, J.R. Bragg, R.M. Atlas, Distribution and weathering of crude oil residues on shorelines 18 years after the Exxon Valdez spill, Environ. Sci. Technol. 42 (2008) 9210–9216.

[3] H.U. Deepthike, R. Tecon, G.V. Kooten, J.R.V.D. Meer, H. Harms, M. Wells, J. Short, Unlike PAHs from Exxon Valdez crude oil, PAHs from Gulf of Alaska coals are not readily bioavailable, Environ. Sci. Technol. 43 (2009) 5864–5870.

[4] N. Jiménez, M. Viñas, J. Sabaté, S. Díez, J.M. Bayona, A.M. Solanas, The Prestige oil spill. 2. Enhanced biodegradation of a heavy fuel oil under field conditions by the use of an oleophilic fertilizer, J. Albaiges, Environ. Sci. Technol. 40 (2006) 2578–2585.

[5] S. Díez, E. Jover, J.M. Bayona, J. Albaigés, Prestige oil spill. III. Fate of a heavy oil in the marine environment, Environ. Sci. Technol. 41 (2007) 3075–3082.

[6] R.M. Atlas, T.C. Hazen, Oil biodegradation and bioremediation: A tale of the two worst spills in U.S. history, Environ. Sci. Technol. 45 (2011) 6709–6715.

[7] Q. Lin, I.A. Mendelssohn, Impacts and recovery of the Deepwater Horizon oil spill on vegetation structure and function of coastal salt marshes in the northern Gulf of Mexico, Environ. Sci. Technol. 46 (2012) 3737–3743.

[8] K. Xia, G. Hagood, C. Childers, J. Atkins, B. Rogers, L. Ware, K. Armbrust, J. Jewell, D. Diaz, N. Gatian, H. Folmer, Polycyclic aromatic hydrocarbons (PAHs) in Mississippi seafood from areas affected by the Deepwater Horizon oil spill, Environ. Sci. Technol. 46 (2012) 5310–5318.

[9] C. Valderrama, X. Gamisans, F.X. de las Heras, J.L. Cortina, A. Farrán, Kinetics of polycyclic aromatic hydrocarbons removal using hyper-cross-linked polymeric sorbents Macronet Hypersol MN200, React. Funct. Polym. 67 (2007) 1515–1529.

[10] D. Ceylan, S. Dogu, B. Karacik, S.D. Yakan, O.S. Okay, O. Okay, Evaluation of butyl rubber as sorbent material for the removal of oil and polycyclic aromatic hydrocarbons from seawater, Environ. Sci. Technol. 43 (2009) 3846–3852.

[11] S.S. Al-Lihaibi, Photo-oxidation products of petroleum hydrocarbons in the Eastern Red Sea coastal waters, Environ. Int. 28 (2003) 573–579.

[12] D.L. Plata, C.M. Sharpless, C.M. Reddy, Photochemical degradation of polycyclic aromatic hydrocarbons in oil films, Environ. Sci. Technol. 42 (2008) 2432–2438.

[13] S.E. Allan, B.W. Smith, K.A. Anderson, Impact of the Deepwater Horizon oil spill on bioavailable polycyclic aromatic hydrocarbons in Gulf of Mexico coastal waters, Environ. Sci. Technol. 46 (2012) 2033–2039.

[14] H.M. Jin, J.M. Kim, H.J. Lee, E.L. Madsen, C.O. Jeon, Alteromonas as a key agent of polycyclic aromatic hydrocarbon biodegradation in crude oil-contaminated coastal sediment, Environ. Sci. Technol. 46 (2012) 7731–7740.

[15] T.R. Annunciado, T. Sydenstricker, S.C. Amico, Experimental investigation of various vegetable fibers as sorbent materials for oil spills, Mar. Pollut. Bull. 50 (2005) 1340–1346.

[16] E. Witka-Jeżewska, J. Hupka, P. Pieniążek, Investigation of oleophilic nature of straw sorbent conditioned in water, Spill Sci. Technol. Bull. 8 (2003) 561–564.

[17] T. Lim, X. Huang, Evaluation of kapok (*Ceiba pentandra* (L.) Gaertn.) as a natural hollow hydrophobic-oleophilic fibrous sorbent for oil spill cleanup, Chemosphere 66 (2007) 955–963.

[18] S.S. Banerjee, M.V. Joshi, R.V. Jayaram, Treatment of oil spill by sorption technique using fatty acid grafted sawdust, Chemosphere 64 (2006) 1026–1031.

[19] M.O. Adebajo, R.L. Frost, J.T. Kloprogge, O. Carmody, S. Kokot, Porous materials for oil spill cleanup: A review of synthesis and absorbing properties, J. Porous Mater. 10 (2003) 159–170.

[20] X. Zhang, C. Wei, Q. He, Y. Ren, Enrichment of chlorobenzene and o-nitrochlorobenzene on biomimetic adsorbent prepared by poly-3-hydroxybutyrate (PHB), J. Hazard. Mater. 177 (2010) 508–515.

[21] X. Zhang, Adsorption/Enrichment of Organochlorine Compounds with Biomimetic Adsorbent Prepared by Poly-3-hydroxybutyrate, South China University of Technology, 2009, pp. 49–87, 127

[22] H. Cao, L. Qin, Experimental study on adsorption properties of diesel oil on exfoliated graphite, J. Wuhan Inst. Chem. Tech. 26 (2004) 38–41.

[23] J. Zhou, T. Tang, M. Zhong, Z. Shen, L. Cui, Adsorption performance of diesel by Kapok Fiber, Environ. Sci. Technol. 33 (2010) 17–20 (in Chinese).

[24] N. Lin, Research on the Modification of Expanded Perlite and Emergency Disposal Technology for Accidental Oil Spill Pollution, Harbin Institute of Technology, Harbin, 2013.

[25] Q. Yang, X. Yi, X. Yu, Q. Guan, Y. Ren, Y. Hu, C. Feng, C. Wei, Biomimetic adsorption of trace amounts of polycylic aromatic hydrocarbonsfrom aqueous solution by poly-3-hydroxybutrate, Environ. Chem. 31 (2012) 1518–1526.

[26] L. Yin, Adsorption of Diesel Oil in Seawater and its Mechanism with Clay Materials and Exfoliate Graphite, Qingdao Technological University, Qingdao, 2009.